MODELING OF CREEP COMPLIANCE AND CREEP MODULUS BEHAVIOR IN MODIFIED ASPHALT MIXES USING ARTIFICIAL NEURAL NETWORKS (ANN) AND ADAPTIVE NEURO-FUZZY INFERENCE SYSTEMS (ANFIS)

Lyacia Sadoudi[1]* – Mohammed Amin Benbouras[1] – RatibaMitiche-Kettab[2]

[1]Departement of Civil Engineering, University of Sciences and TechologyHouariBoumediene, BP 32 El Alia Bab Ezzouar Algiers, Algeria,
[2]Department of Civil Engineering, EcoleNationalePolytechniqued'Alger, Algeria,

ARTICLE INFO

***Article history*:**
Received: 22.02.2024.
Received in revised form: 16.03.2025.
Accepted: 16.05.2025.

Keywords:
Asphalt
Creep properties
Artificial Neural Network (ANN)
Adaptive Neuro-Fuzzy
Inference System (ANFIS).

DOI: https://doi.org/10.30765/er.2464

Abstract:

This study investigates the impact of rubber on the creep compliance and creep modulus of asphalt mixtures, aiming to enhance their mechanical performance and promote environmental sustainability. Rubber was incorporated into the asphalt mixture using the dry process. Asphalt samples were prepared using different content of rubber both the gyratory compactor and the Marshall Method and tested at different temperatures. The results showed that adding a low percentage of rubber (0.25%) improved creep modulus and reduced deformation, while higher percentages led to decreased performance. Additionally, the study utilized advanced machine learning techniques, including Artificial Neural Networks (ANN) and Adaptive Neuro-Fuzzy Inference Systems (ANFIS), to model creep modulus and creep compliance. The ANFIS model demonstrated superior performance in predicting these properties compared to the ANN model. The findings of this research provide valuable insights into the influence of rubber on the creep behavior of asphalt mixtures and offer a robust framework for predicting their performance using machine learning techniques.

1 Introduction

The use of polymer as a modifier in asphalt mixtures has gained increasing attention due to its potential to enhance mechanical performance and promote sustainability in pavement engineering [1]. Asphalt mixtures are subjected to repeated traffic loading and temperature variations, leading to permanent deformations such as rutting [2]. One of the critical parameters in evaluating the durability of these mixtures is creep stiffness, which measures their ability to resist deformation under sustained loading. In Algeria, rubber waste—such as tires, shoe soles, and vehicle carpets—constitutes a significant challenge in solid waste management. To address this issue and add value to this waste, several researchers in the field of public works have proposed solutions aimed at both protecting the environment from the hazards posed by this waste and enhancing the performance of bituminous mixtures used in wearing courses. Due to pavement degradation caused by high temperatures and heavy traffic, researchers have proposed two types of modifications to enhance the performance of bituminous mixtures. The wet process, where additives are mixed directly into the bitumen, and the dry process, where additives are added directly into the asphalt mixture. Numerous studies have been conducted on modified asphalt mixtures to enhance their performance in terms of stiffness, stability, fatigue resistance, and creep behavior. Asphalt specimens with polystyrene contents of 0%, 5%, 10%, 15%, and 20% by binder volume were tested at three temperatures (25°C, 40°C, and 55°C). The findings indicate that higher polystyrene content leads to faster strain increase and greater permanent deformation at high temperatures (55°C). However, increased polystyrene content also improves stiffness at higher temperature [3]**.** The results of the static creep behavior of bituminous mixes modified with (0%, 1%, 3%, 5%) FORTA-FI fibers subjected to different compaction forces (35, 50 and 75 blows) and temperatures (25 °C, 40 °C, 55 °C) showed that with

the increase in temperature, the accumulated micro-strain also increased, while the stiffness modulus decreased, which is consistent with the viscoelastic nature of bituminous mixes. In addition, a predictive model was developed using artificial neural networks (ANN) to relate the strain and stiffness modulus to variables such as temperature, fiber content and compaction force, thus achieving a high result [4]. Due to the increased use of recycled materials such as RAP and RAS, a study of thermal cracking of flexible pavements in the northern United States and Canada was developed. This study critiques the Pavement ME Design (MEPDG) model, which overestimates creep compliance, especially when recycled materials are involved. The research proposes a new model that better accounts for recycled materials and asphalt binder replacement (ABR), showing increased accuracy in predicting pavement performance. The model was validated by laboratory data, demonstrating a strong correlation [5]**.** Two asphalt binders, CAP 50/70 and AMP 60/85, were used to examine the mechanical behavior of hot mix asphalts with respect to permanent deformation using static creep tests and Superpave compaction curve parameters. The results show that asphalts containing the CAP 50/70 binder exhibit better workability and lower deformation. Also, the use of a higher binder content results in greater permanent deformation, but better workability.

The study identifies strong correlations between compaction indices and static creep test results, suggesting that these indices can predict the behavior of the asphalt mix with respect to permanent deformation [6]. A method for calculating the relaxation modulus of bituminous mixes by Laplace transform was developed. It consists of performing uniaxial static creep tests on four bituminous mixes at different temperatures and modeling the creep compliance using the Prony series and the power law. The relaxation modulus is derived from the creep compliance by Laplace transform, the results being validated by two methods: Simpson and Gauss. The study introduces a more efficient and accurate method, using the fixed Talbot method for numerical inversion, 25 times faster than the Gauss method, thus providing a powerful tool for the interconversion of viscoelastic functions of bituminous mixes. The results of using recycled polyethylene terephthalate (PET) fibers at different percentages (0.3%, 0.5%, 0.7% and 1.0%) to improve the performance of asphalt concrete by increasing its resistance to fatigue cracking and rutting indicate that mixtures containing 0.5% PET fibers provided the most significant improvements, improving resistance to permanent deformation, increasing the modulus of resilience and increasing resistance to fatigue and rutting, making it the optimal fiber content for asphalt mixtures [7]. To predict the creep rate as a function of rubber content, temperature, compaction, and load stress of modified asphalt concrete with different rubber contents, a multi-layer backpropagation network model was developed based on experimental data.

The results show that a 2% polymer addition reduces the creep rate, but higher percentages do not further reduce the permanent deformation. The ANN model has been shown to be effective for the design of modified asphalt concrete, with accurate predictions and a low error rate [8]. The results of the study of the use of low-density polyethylene (LDPE) plastic waste as an additive to improve the creep and recovery behavior of bituminous mixes showed that the addition of 5% LDPE improves the thermomechanical performance of the mix, reducing the total deformation by 51% at 20 °C and by 13% at 50 °C. This modification improves resistance to permanent deformation, stiffness and durability, providing an economical and ecological solution for road construction, especially in hot Saharan regions where service temperatures are high [9]. Two predictive models to improve the prediction of asphalt mixtures' creep compliance performance were utilized : one using multiple regression analysis and the other utilizing feed-forward artificial neural networks (ANN). The models were assessed based on factors like loading time, testing temperature, asphalt modification, air voids level, and aging conditions. The findings reveal that the ANN model significantly outperforms the regression model in prediction accuracy, explaining over 99% of the measured data, making it a promising tool for efficiently selecting asphalt mixture variables with minimal error [10]. Furthermore, other studies have achieved notable success in using machine learning methods to model creep modulus and creep compliance in asphalt mixtures. Among the most influential studies, Zofka and Yut (2012) employed a one-hidden-layer artificial neural network (ANN) model with selected input parameters to model asphalt creep compliance, achieving a high correlation of 97 to 99 percent between predicted and measured values [11]. Liu and Liu (2021) predicted low-temperature creep compliances of asphalt mixtures using both multiple linear regression and ANN after analyzing a dataset of 1,890 samples [12]. Their models significantly outperformed existing methods, delivering much higher prediction accuracy [12]. Similarly, Roshan and Abdelrahman (2024) applied ANN to estimate flexural-creep modulus, demonstrating a high coefficient of determination (near 90%) for their proposed model [13]. However, the models previously discussed in the literature have been primarily limited to multiple regression analysis and artificial neural networks.

This study introduces two key contributions. First, it successfully investigates the effect of rubber—derived from recycled materials like shoe soles and vehicle carpets—on the static creep behavior of asphalt mixtures. Rubber was integrated into the asphalt mixture using the dry process, and the asphalt samples were compacted using both the gyratory compactor and the Marshall method before being subjected to a compressive stress of 0.14 MPa. Second, the study provides new alternative models for predicting creep modulus and creep compliance in asphalt mixtures by applying two advanced machine learning techniques for the first time: artificial neural networks (ANN) and the adaptive neuro-fuzzy inference system (ANFIS). Moreover, the study uses several high-performance indicators—such as mean absolute error (MAE), root mean square error (RMSE), coefficient of determination (R^2), and Pearson correlation coefficient (R)—to assess the generalization capability of the learning models and compare the predictive capabilities of the two methods.

2 Materials

2.1 Aggregates and bitumen

In this study, sand (0/3) and limestone gravel (3/8, 8/15) were utilized to prepare asphalt concrete mixtures. These aggregates are from the KADDARA quarry, located in Boumerdes, Algeria and are commonly employed in the construction of flexible pavements. Prior to mixture preparation, the aggregate quality was evaluated and found to meet the specifications outlined by the Ministry of Road Transport and Highways guidelines. The mechanical properties of the aggregates used are presented in Table 1.

Table 1. Properties of mineral aggregate.

Properties	Test method	Fraction			Specifications
		0/3	3/8	8/15	
Specific gravity (g/cm3)	NA P 18-555	2.71	2.67	2.69	>2.6
Los Angeles coeff (%)	EN 1097-2	-	-	24.3	20 <LA<30
Micro deval (%)	EN 1097-2	-	13.6	19.8	20 <ME<25
Sand equivalent (%)	EN 933-8	56	-	-	≥ 60
Flattening coeff (%)	EN 933-3	-	9.8	12.5	< 25

2.2 Asphalt binder

The study employed a 40/50 penetration-grade bitumen, procured from the Algerian oil refining company NAFTAL, with its properties outlined in Table 2.

Table 2. Properties of bitumen.

Properties	Test method	Value	Specifications
Penetration (25°, 0.1mm)	EN 1426	43.63	40-50
Softening point, C°	EN 1427	53.25	50-58
Flash point C°	EN ISO 2592	300	> 250°
Ductility (cm)	NA 5223	>100	>100
Specific gravity (25C°) g/Cm3	NF T 66-007	1.039	1-1.1

2.3 Rubber

Characterization of the rubber was conducted using Fourier Transform Infrared (FTIR) spectroscopy, Scanning Electron Microscopy (SEM), and Energy Dispersive Spectroscopy (EDS). The size of the rubber is (0.1 to 2mm) [14], [15]. FTIR analysis suggests that the rubber primarily consists of styrene-butadiene-styrene (SBS) combined with zinc oxide. The SEM analysis revealed that the material has a dense and heterogeneous structure [16].

3 Samples preparation and Methods

3.1 Agregate gradation and samples

The optimal aggregate-bitumen mixture was determined through multiple iterations of aggregate and bitumen percentage combinations. This process involved the use of the gyratory compactor test to evaluate and refine the mix design. Several trials were conducted to ensure that the final blend met the required specifications set by the standard. The selected mixture demonstrated satisfactory performance in terms of density, void content, and mechanical properties, ensuring compliance with the established criteria for durability and stability. Samples for both control and modified mixtures were prepared by combining the optimum asphalt binder content (5.76%) with the specified percentage of rubber and aggregates, using the dry process. The mixtures were heated to 160°C and thoroughly mixed to ensure uniform coating of the aggregates. They were then kept in an oven at 160°C for 120 minutes, a duration confirmed to be sufficient for achieving complete interaction between the rubber and the bitumen [17], [18], [19]. Static creep tests were performed on various asphalt mixtures at two temperatures, 20°C and 60°C, using samples compacted with both the Marshall Hammer and the gyratory compactor.

3.2 Visco-deformation test

This test involves subjecting asphalt mixture samples (0/14 grading), including control and modified mixtures with rubber contents of 0.25%, 0.5%, and 0.75%, to a compressive stress of 0.14 MPa. The test was conducted at two temperatures, 20°C and 60°C. After preparation, the samples were left to rest for 24 hours and then conditioned at the test temperature for 4 hours. The test consisted of two phases: a loading phase lasting 1 hour and an unloading phase of the same duration. The following parameters were recorded during the test: total deformation (ε_{Tot}), initial deformation (ε_{In}), permanent deformation (ε_{Per}), creep modulus, and creep compliance.

3.3 Artificial neural network

An artificial neural network (ANN) is a form of artificial intelligence inspired by the intricate workings of the human brain. It is defined as a network of interconnected units, often referred to as "processing elements" (PEs), "nodes," or "units," arranged in multiple layers: an input layer, an output layer, and one or more hidden layers in between. Each node in a given layer is either fully or partially connected to various PEs in the other layers through a modeling process [20].

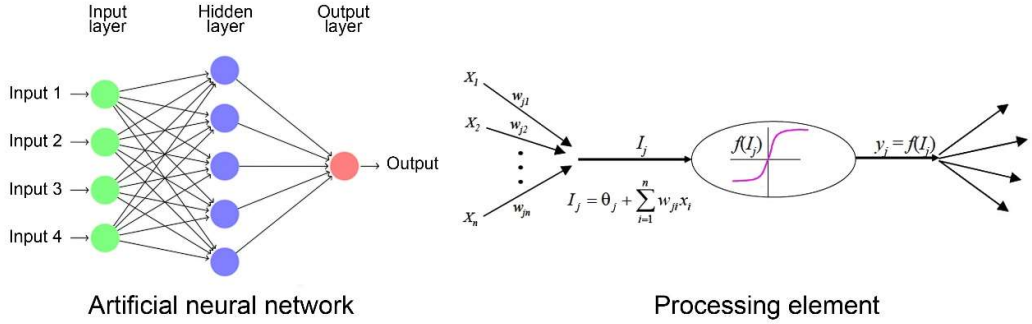

Figure 1. A structure of typical ANN.

The ANN modeling process involves multiplying each node in the previous layer by an adjustable connection weight (Wji). At each processing element (PE), the weighted input signals are summed, and a threshold value (θ_i) is added [20] The total sum is then passed through a transfer function, which is selected based on the nature of the problem the network aims to solve (e.g., linear, log-sigmoid, or tan-sigmoid functions) [21]. This procedure is outlined in Eq. 1 and Eq. 2, as shown in Figure 1.

$$I_j = \sum W_{ji} X_i + \theta_i \tag{1}$$

$$y_j = f(I_j) \tag{2}$$

The fundamental concept of artificial neural networks (ANNs) involves three primary phases: training, testing, and validation. The objective is to minimize the discrepancy between predicted and actual values. During the training phase, weights and biases are iteratively adjusted, typically using the widely adopted "Backpropagation Algorithm," until specific stopping criteria are met. Ultimately, the system generates an optimized model, defined by its weights and biases matrix, capable of accurately predicting target values from input data with minimal error [22], [23].

3.4 Adaptive neuro fuzzy inference system

The Adaptive Neuro-Fuzzy Inference System (ANFIS) integrates the capabilities of an adaptive Artificial Neural Network (ANN) with those of a Fuzzy Inference System (FIS)[24]. Introduced by Jang in 1993, ANFIS has proven effective in solving nonlinear problems, as evidenced by numerous studies. By training on input-output data, the system optimizes the parameters of its Membership Functions (MFs)[24]. The ANFIS structure, depicted in Figure 2, is composed of five layers. The first layer, known as the fuzzification layer, transforms input variables into fuzzy membership functions at each node j using an activation function μ. These functions can take various forms, including triangular, trapezoidal, sigmoidal, and Gaussian shapes, as defined by Equations 3 and 4[24].

$$Q_j^1 = \mu_{Aj}(x) \text{ for } j = 1, 2 \tag{3}$$

$$Q_j^1 = \mu_{Bj-2}(y) \text{ for } j = 3, 4 \tag{4}$$

Where x and y are the inputs, Q_j^1 is the membership function, and Aj and Bj are the membership values of μ. In the current study, the Gaussian membership function presented in Equation. 3 has been used,

$$\mu(x) = \exp\left[-\left(\frac{(x-c_j)^2}{2\sigma_j^2}\right)\right] \tag{5}$$

The parameters *Cj* and *σj*, representing the mean and standard deviation of the Gaussian curve, respectively, act as the premise parameters for the membership functions. In the second layer, the weights (wk) of these membership functions are calculated using Equation 6, which determines the firing strength of the associated rules.

$$Q_k^2 = w_k = \mu_{Aj}(x) * \mu_{Bj}(y) \qquad \text{for } k=1,\ldots..,\ 4 \text{ and } j = 1, 2 \tag{6}$$

The layer 3 normalizes the firing strengths using Equation 5.

$$Q_j^3 = \overline{w}_j = \frac{w_j}{\sum_{k=1}^{4} w_k} \qquad \text{for } j=1, .., 4 \tag{7}$$

In layer 4, known as the defuzzification layer, the output for each node *j* is evaluated using Equation 8, and the consequent parameters (*p*, *q*, and *r*) of the firing strengths *f* are calculated.

$$Q_j^4 = \overline{w}_j f_j = \overline{w}_j (p_j x + q_j y + r_j) \qquad \text{for } j=1, .., 4 \tag{8}$$

The final layer calculates the overall output in a single node by summing up all the incoming signals, as described by Equation 9.

$$Q_j^5 = \sum \overline{w}_j f_j = \frac{\sum_{j=1}^{4} w_j f_j}{\sum_{j=1}^{4} w_j} \tag{9}$$

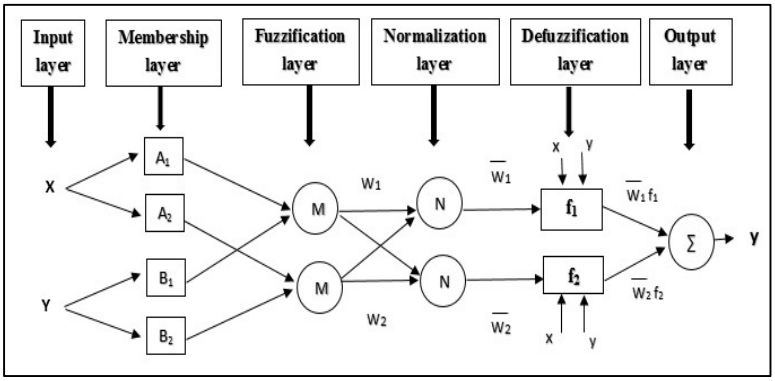

Figure 2. Architecture of ANFIS model.

3.5 Statistical Performance Indicators

The accuracy of the proposed models was evaluated using various statistical performance metrics and graphical analysis. The statistical indicators included the Mean Square Error (MSE), Root Mean Square Error (RMSE), Coefficient of Determination (R^2), and Pearson Correlation Coefficient (R). These metrics are defined as follows [25], [26]:

Mean Square Error (*MAE*):

$$MSE = \frac{1}{N}\sum_{i=1}^{N}\left(Y_{tar,i} - Y_{out,i}\right)^2 (0 < RMSE < \infty) \tag{10}$$

Root Mean Square Error (*RMSE*):

$$RMSE = \sqrt{\frac{1}{N}\sum_{i=1}^{N}\left(Y_{tar,i} - Y_{out,i}\right)^2} (0 < RMSE < \infty) \tag{11}$$

Pearson correlation coefficient (R):

$$R = \frac{\sum_{i=1}^{N}\left(\left(Y_{tar,i} - \overline{Y_{tar}}\right)\left(Y_{out,i} - \overline{Y_{out}}\right)\right)}{\sqrt{\sum_{i=1}^{N}\left(\left(Y_{tar,i} - \overline{Y_{tar}}\right)^2\left(Y_{out,i} - \overline{Y_{out}}\right)^2\right)}} (-1 < R < 1) \tag{12}$$

Coefficient of determination (R^2):

$$R^2 = 1 - \frac{\sum_{i=1}^{N}\left(Y_{tar,i} - Y_{out,i}\right)^2}{\sum_{i=1}^{N}\left(Y_{tar,i} - \overline{Y_{tar}}\right)^2} (0 < NSE < 1) \tag{13}$$

4 Results

Permanent deformation behavior of both control and modified asphalt mixtures was evaluated at 20°C and 60°C using both Marshall and gyratory compaction methods. The study focused on the following parameters: initial deformation (ε_{EC}) measured after 15 seconds of loading, maximum deformation (ε_{max}) recorded after 1 hour of loading, permanent or residual deformation (ε_{Res}), creep modulus, and creep compliance.

4.1 Effect of temperature and rubber on parameters of visco-deformation

This section investigates the influence of temperature (20°C and 60°C) and rubber content (0%, 0.25%, 0.5%, and 0.75%) on the visco-deformation behavior of asphalt mixtures. The analysis focuses on key parameters such as compressive strain, creep modulus, and compliance modulus, considering samples compacted using both the gyratory compactor and the Marshall method.

4.1.1 Compressive strain

The compressive strain values are determined as the ratio of the recorded deformations to the initial height of the specimen. This ratio is calculated using the following equation:

$$\varepsilon(t) = \Delta h/ho \tag{14}$$

The values of various compressive strain recorded during one hour of loading and one hour of unloading are shown in Figure 3. The creep-recovery curves in Figure 3 illustrate the impact of rubber and temperature on the axial micro-deformation of asphalt mixtures over time at both medium and high temperatures (20°C and 60°C).

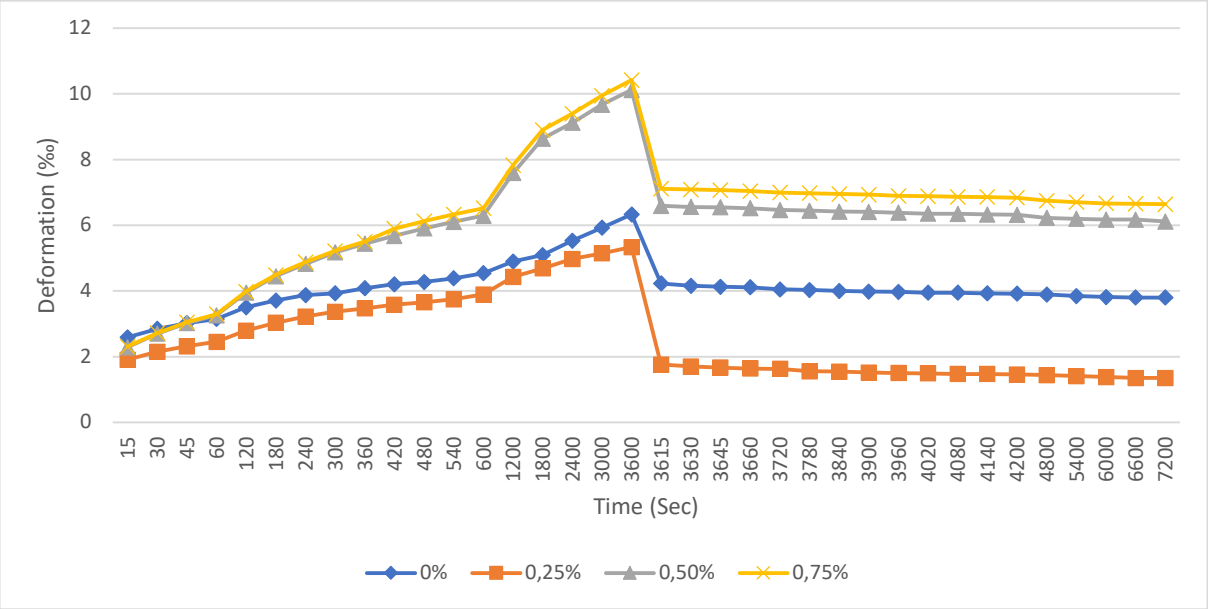

4.a) Compressive strain at 20°C with gyratory compactor.

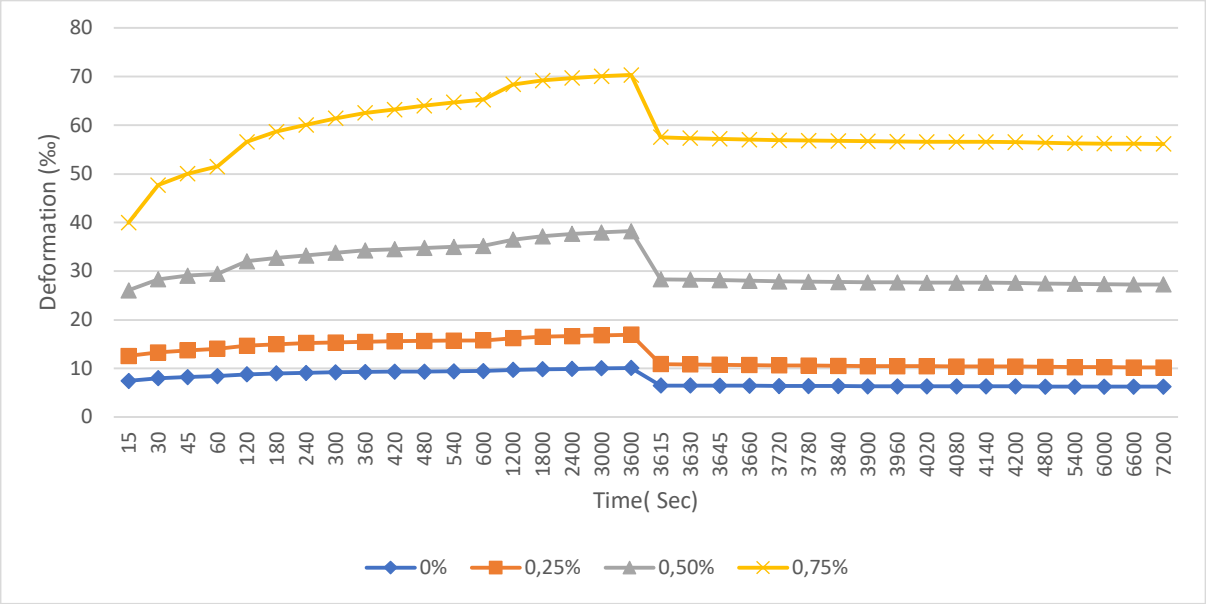

4.b) Compressive strain at 60°C with gyratory compactor.

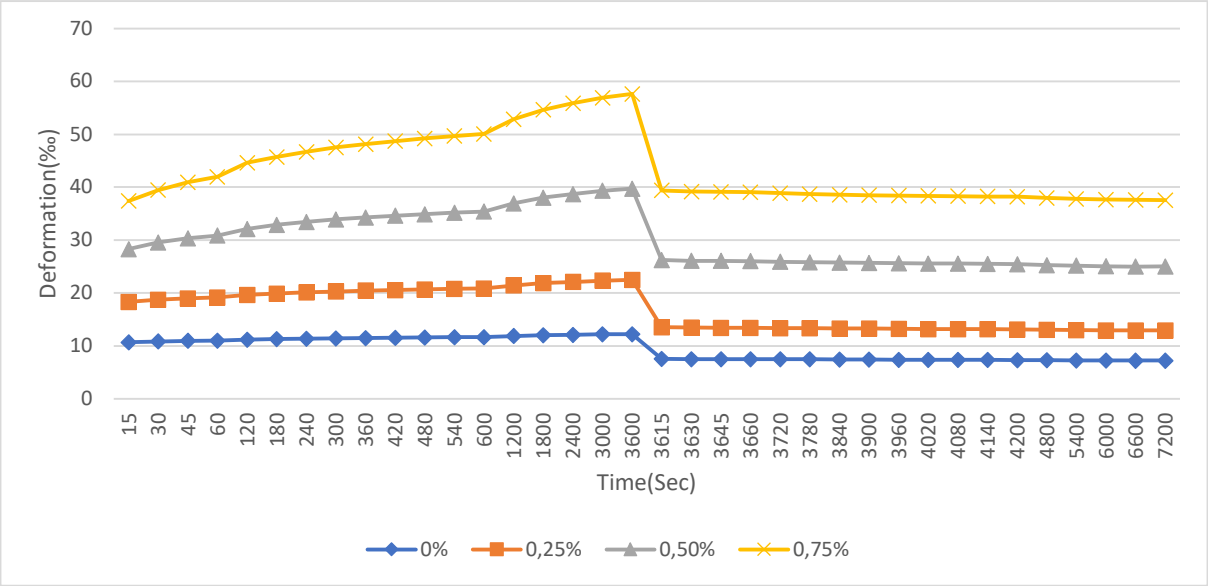

4.c) Compressive strain at 20°C with Marshall Method.

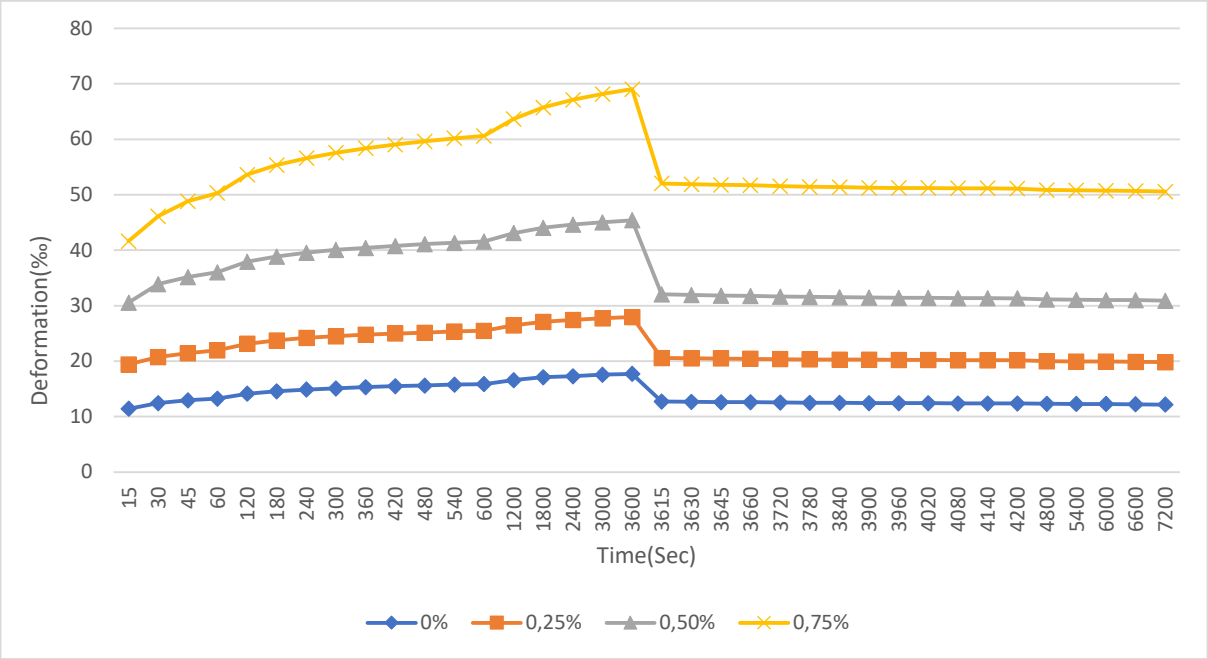

4.d) Compressive strain at 60°C with Marshall Method.

Figure 3. Compressive strain at 20°C and 60°C with gyratory compactor and Marshall Method for control and modified mixtures: a) Compressive strain at 20°C with gyratory compactor, b) Compressive strain at 60°C with gyratory compactor, c) Compressive strain at 20°C with Marshall Method, d) Compressive strain at 60°C with Marshall Method.

The results indicate that compressive strain increase with rising temperature for the control mixture. At higher temperatures, the recorded deformations are greater than at moderate temperatures. For samples compacted with a gyratory compactor, the initial deformation at 20°C is 2.59‰, which is almost three times smaller than the value at 60°C, which is 7.43‰. This difference is attributed to the elastic behavior of the material at elevated temperatures. Conversely, for samples compacted with the Marshall method, the initial deformation at 60°C is only 7% higher than at 20°C. Additionally, for samples compacted with a gyratory compactor, the maximum deformation at 20°C increases almost 2.5 times compared to the initial deformation. At 60°C, the increase is smaller, about 35% more than at 20°C. For the Marshall method samples, the maximum deformation increases by 14% at 20°C and 54% at 60°C. During the recovery phase, samples compacted with the gyratory compactor recover about 40% of the maximum deformation at 20°C, reflecting the elastic behavior of the asphalt mixtures. At 60°C, the permanent deformation represents 62% of the maximum deformation, indicating the viscoelastic nature of the asphalt.

The recovery rate for samples compacted using the Marshall method is similar to that of the gyratory compactor samples. Moreover, the results reveal that the visco-deformation for Marshall compacted samples occurs predominantly during the initial phase (about 80% at 20°C and 64% at 60°C of the maximum deformation). For samples compacted with a gyratory compactor, the visco-deformation takes place mainly in the final phase (about 60% of the maximum deformation at 20°C), but at 60°C, the creep deformation is observed in the initial phase. At 20°C, the modified samples compacted with a gyratory compactor containing 0.25% rubber show a 26% reduction in initial axial deformation and a 15.63% reduction in maximum deformation compared to the control mixture. At 60°C, both initial and maximum deformations decrease by about 30% compared to the control mixture. For samples compacted with the Marshall method, the initial deformation decreases by 29% at 20°C and 30% at 60°C, and the maximum deformation decreases by 42% at 60°C compared to 16% at 20°C. Mixtures containing 0.5% and 0.75% rubber exhibit significant increases in deformation. At both temperature levels (20°C and 60°C), the mixtures with 0.25% rubber show better creep performance, resulting in lower axial deformations. Conversely, the highest axial deformations are observed

for mixtures with 0.5% and 0.75% rubber. The reduction in axial deformation for the 0.25% rubber mixture is likely due to the presence of zinc oxide in the additive, which acts as a particle-agglomerating agent. Additionally, the rubber functions as a dopant, strengthening the bond between the mixture components. On the other hand, the increased axial deformation for mixtures with 0.5% and 0.75% rubber is likely caused by unabsorbed crumb particles, which disrupt the binder continuity and the bond between the components. It is also noted that mixtures compacted with a gyratory compactor exhibit lower axial deformations at lower temperatures compared to those compacted with the Marshall method, leading to better resistance to rutting. Overall, axial deformations recorded during the creep test are higher for samples compacted with the Marshall method compared to those compacted with the gyratory compactor.

4.1.2 Creep modulus.

The stiffness of asphalt mixtures plays a vital role in evaluating their mechanical performance. It reflects the material's capacity to withstand and distribute stress when subjected to a load. Creep modulus was evaluated using two factors: the compressive stress applied to the samples (σ) and the deformation observed during the two-hour testing period (ε(t)). The creep modulus was then calculated using the following equation:

$$Sm = \frac{\sigma_0}{\varepsilon_{(t,T)}} \tag{15}$$

Figure 4 shows the variation in creep modulus modulus as a function of the rubber percentage for samples compacted using the Gyratory Compactor and the Marshall Method at temperatures of 20°C and 60°C.

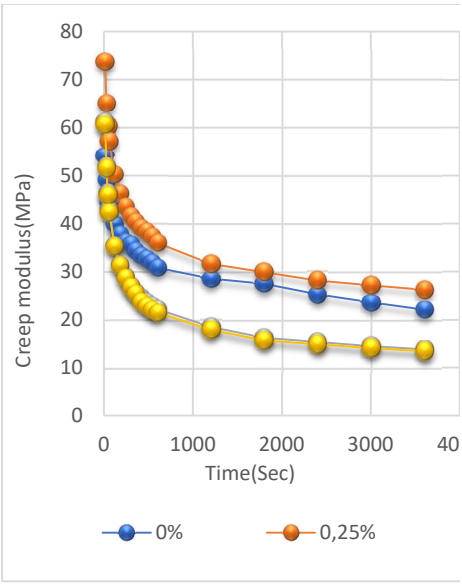

a) Creep modulus at 20°C with gyratory compactor

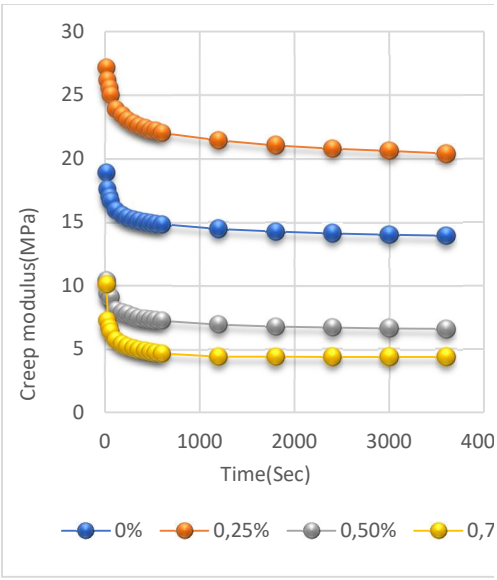

b) Creep modulus at 60°C with gyratory compactor

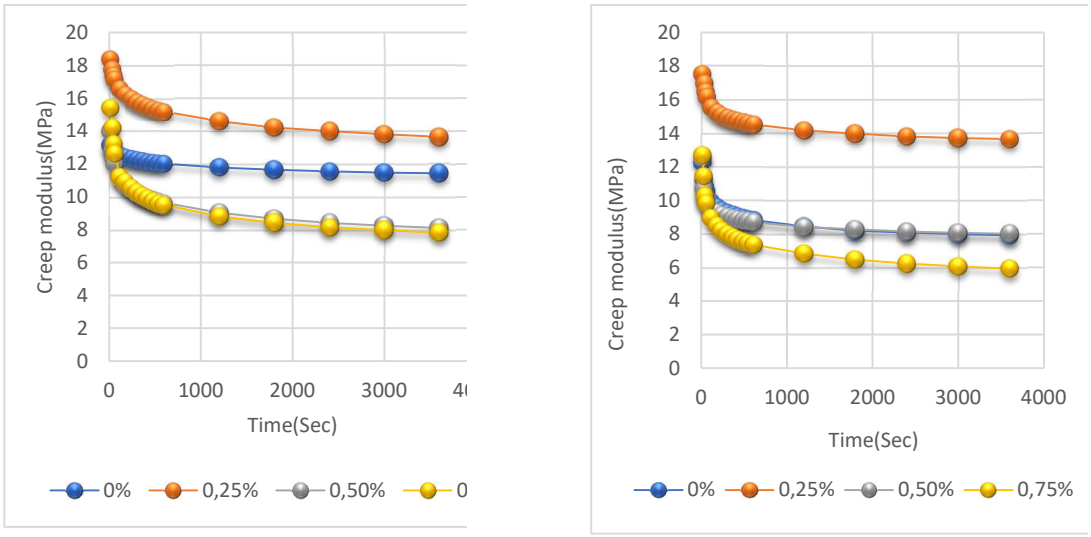

c) Creep modulus at 20°C with Marshall Method *d) Creep modulus at 60°C with Marshall Method*

Figure 4. Creep modulus at 20°C and 60°C with gyratory compactor and Marshall Method for control and modified mixtures: a) Creep modulus at 20°C with gyratory compactor, b) Creep modulus at 60°C with gyratory compactor, c) Creep modulus at 20°C with Marshall Method, d) Creep modulus at 60°C with Marshall Method.

The results indicate that adding rubber to the control mixture increases the creep modulus for the mix containing 0.25% rubber. However, mixtures with 0.5% and 0.75% rubber show a reduction in creep modulus compared to the control. Additionally, creep modulus decreases with increasing temperature. At both 20°C and 60°C, the samples with 0.25% rubber, compacted using the Gyratory Compactor, exhibited the highest creep modulus values, while the lowest values were observed in the samples with 0.75% rubber. Furthermore, a 46% and 70% increase in creep modulus was noted for samples containing 0.25% of rubber, compacted with the Gyratory Compactor and the Marshall Method, respectively. The reduction in stiffness for mixtures with higher rubber content may be attributed to the weak bond between the bituminous binder and the rubber particles. For all rubber percentages, the stiffness decreases with increasing temperature, showing an optimum at 0.25% rubber. This behavior can be explained by the elastic properties of rubber, which enhances the elasticity of the bituminous mix. Additionally, the temperature sensitivity of the bituminous binder, which becomes less stiff and viscous as temperature rises, contributes to the mixture's improved resistance to permanent deformations.

4.1.3 Creep compliance

In this study, characterizing the viscoelastic behavior of the mixtures requires determining their creep compliance, which is a crucial parameter in creep testing. Creep compliance, represented as D(t), is the reciprocal of the creep modulus modulus. It is computed by dividing the axial deformation by the applied stress.

$$D(t) = \frac{\varepsilon_{(t,T)}}{\sigma} \tag{16}$$

Where D (t) is the creep compliance at any time t (1/MPa), $\varepsilon_{(t,T)}$ is the axial deformation at any time t, and σ is the axial constant stress (MPa). Figure 5 illustrates the change in creep compliance over one hour of loading for both conventional and modified asphalt mixtures, as a function of time, at medium (20°C) and high (60°C) temperatures. The mixtures include varying amounts of rubber and were compacted using both the gyratory compactor and Marshall method.

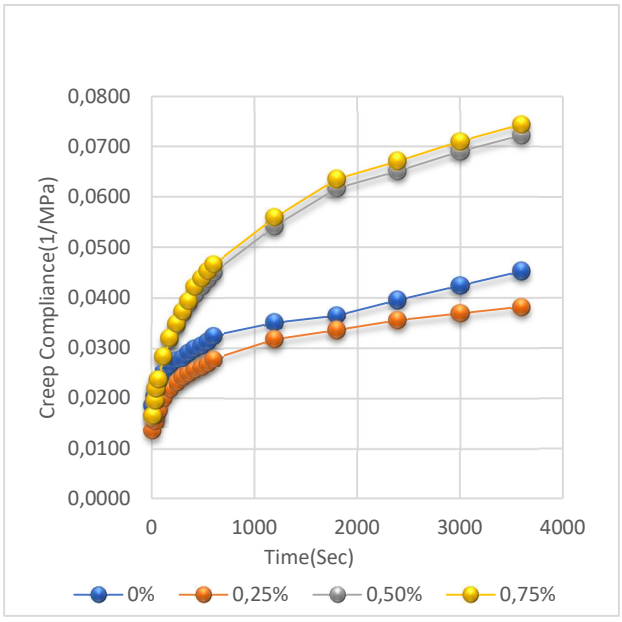

a) Creep compliance at 20°C with gyratory compactor

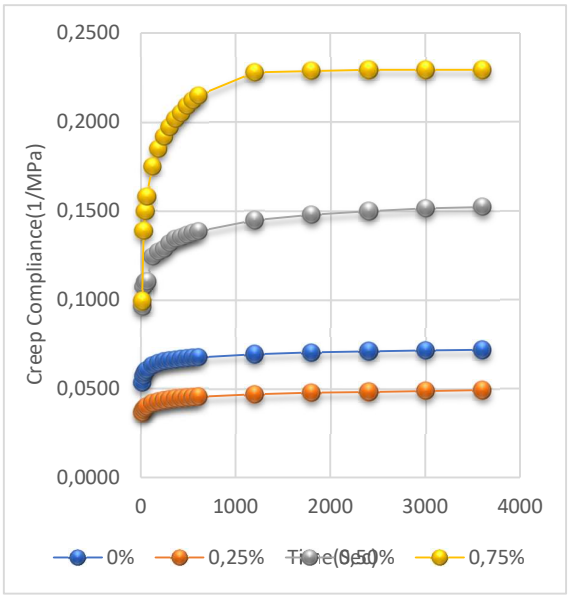

b) Creep compliance at 60°C with gyratory compactor

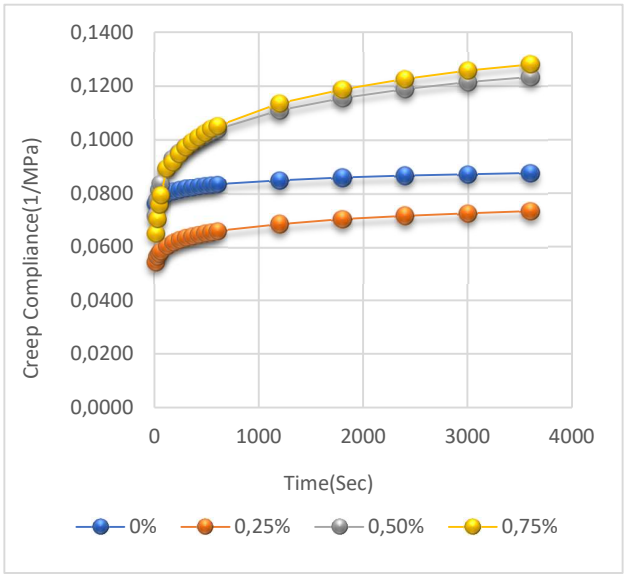

c) Creep compliance at 20°C with Marshall Method

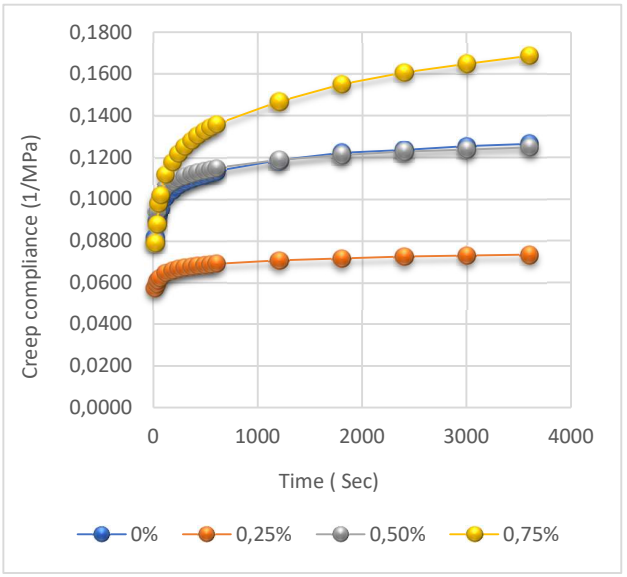

d) Creep compliance at 60°C with Marshall Method

Figure 5. Creep compliance at 20°C and 60°C with gyratory compactor and Marshall Method for control and modified mixtures: a) Creep modulus at 20°C with gyratory compactor, b) Creep modulus at 60°C with gyratory compactor, c) Creep modulus at 20°C with Marshall Method, d) Creep modulus at 60°C with Marshall Method.

The results shown in Figure 5 indicate that the addition of rubber to asphalt mixtures reduces the creep compliance values. At medium temperature, the creep compliance decreases for both compaction methods, leading to improved resistance to permanent deformations (rutting) in the mixtures. Additionally, the creep compliance values are higher for samples compacted using the Marshall method compared to those compacted with the gyratory compactor. At 20°C and 60°C, samples compacted with the gyratory compactor containing 0.25% rubber show a decrease in creep compliance by approximately 15% and 31%, respectively. In contrast,

mixtures containing 0.5% and 0.75% rubber exhibit a notable increase in creep compliance. For the samples compacted using the Marshall method, similar trends in creep compliance were observed as with the gyratory compactor, with a decrease of about 16% and 41% at 20°C and 60°C, respectively, for the mixture containing 0.25% rubber compared to the control mixture. At 60°C, a significant increase in creep compliance was noted for the mixture containing 0.75% rubber, relative to the control mixture. These findings are consistent with the results of deformation and stiffness observed earlier.

4.2 Artificial Neural Network (ANN)

In this study, ANN and ANFIS model was developed to creep modulus (Y1) and creep Compliance (Y2) of modified asphalt mixtures, using Matlab. Table 4 presents the inputs and targets used in ANN and ANFIS modelling.

Table 3. Inputs and targets used in ANFIS modelling.

Inputs	Rubber content.	X1
	Axial micro-deformation (‰).	X2
Targets	Creep modulus.	Y1
	Creep Compilance.	Y2

To identify the most suitable ANN model, the process involves two primary steps: selecting the input parameters and determining the optimal number of nodes in the hidden layer. First, the appropriate input parameters for evaluating Y1 and Y2 were chosen by training ANN models based on the empirical rule proposed by Kanellopoulos and Wilkinson (1997). According to their findings, the optimal number of nodes in a single hidden layer is approximately twice the number of input parameters. Subsequently, ANN models were trained using various combinations of input parameters, with the number of nodes in the hidden layer fixed according to this empirical rule. In the second step, the optimal number of nodes for evaluating. Y1 and Y2 was determined by minimizing the Mean Square Error (MSE) and maximizing the correlation coefficient (R) for the validation data. While numerous studies propose different empirical methods for identifying the optimal number of hidden layers and nodes, the trial-and-error method remains the most accurate and effective, despite being time-intensive (Shahabian, Elachachi, and Breysse, 2014).

At this stage, the trial-and-error approach was applied by varying the network architecture and calculating the correlation coefficient and MSE for each configuration to identify the best model. A single hidden layer with 0–10 nodes was explored, and the optimal performance was achieved with 7 neurons in the hidden layer, resulting in a network structure of 2-7-2. It is worth noting that the tan-sigmoid function served as the transfer function for both layers in the optimal ANN model. Figures 8 to 11 illustrate the relationship between measured (target) and predicted (output) values for Y1 and Y2 using both the Gyratory Compactor and Marshall Method. These figures demonstrate a strong correlation between training and validation data, with R=0.976 for Y1 and R=0.984 for Y2 using the Gyratory Compactor. Similarly, the Marshall Method yielded high-performance results with R=0.961 for Y1 and R=0.950 for Y2. These results indicate that the proposed ANN model delivers high performance, with predictions closely aligned with experimental outcomes, further validating its effectiveness.

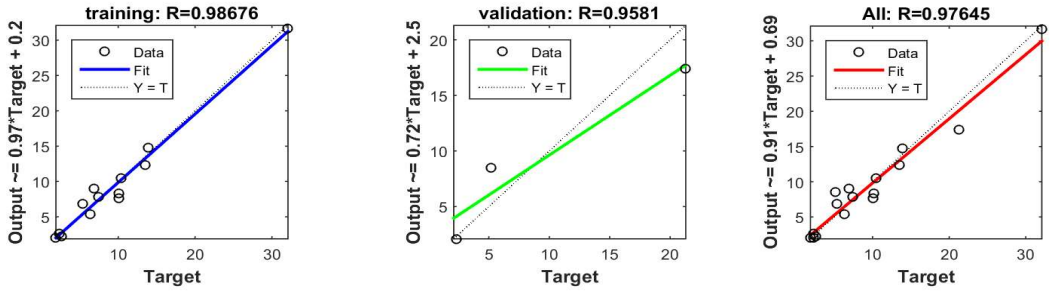

Figure 6. Relation between predicted and measured Y1 based on Gyratory compactor using ANN.

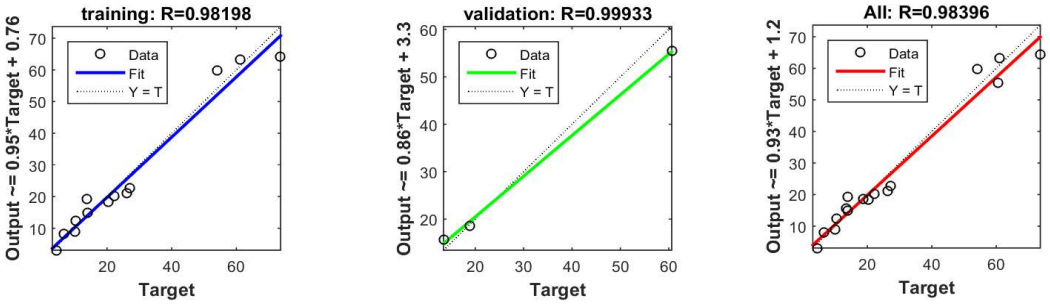

Figure 7. Relation between predicted and measured Y2 based on Gyratory compactor using ANN.

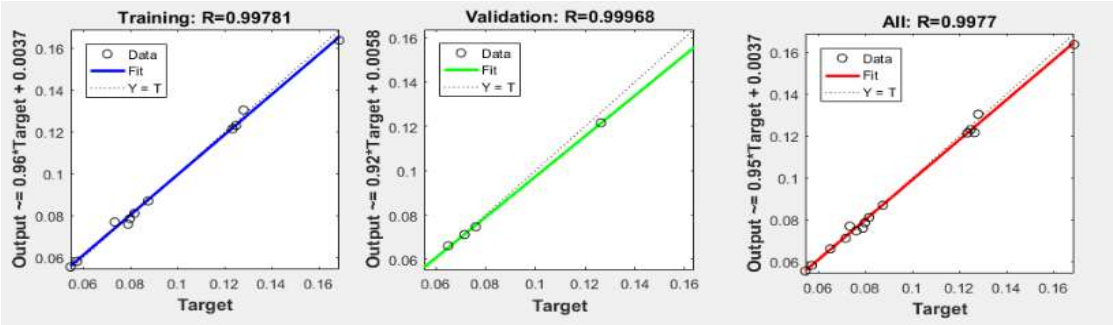

Figure 8. Relation between predicted and measured Y1 based on Marshall method using ANN.

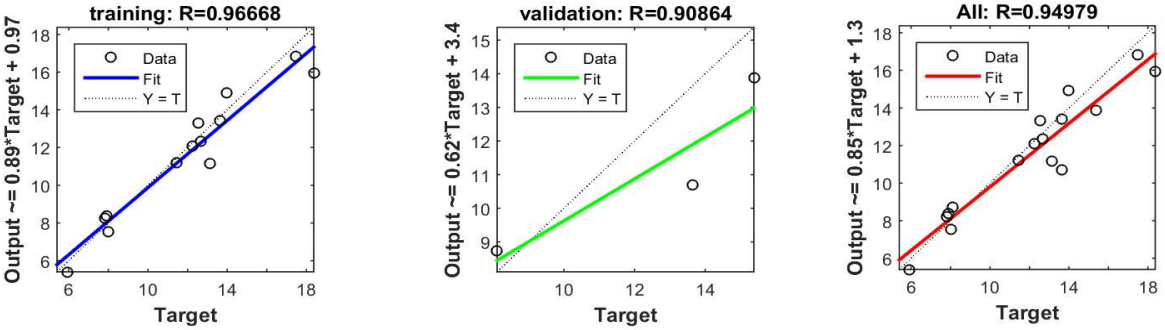

Figure 9. Relation between predicted and measured Y2 based on Marshall method using ANN.

4.3 Adaptive Neuro-Fuzzy Inference System (ANFIS)

In this study, an ANFIS model was developed to creep modulus (Y1) and creep Compliance (Y2) of modified asphalt mixtures, using ANFIS interface within matlab software. Table 4 presents the inputs and targets used in ANFIS modelling. Figure 12 presents the architecture of the ANFIS model with inputs and outputs parameters.

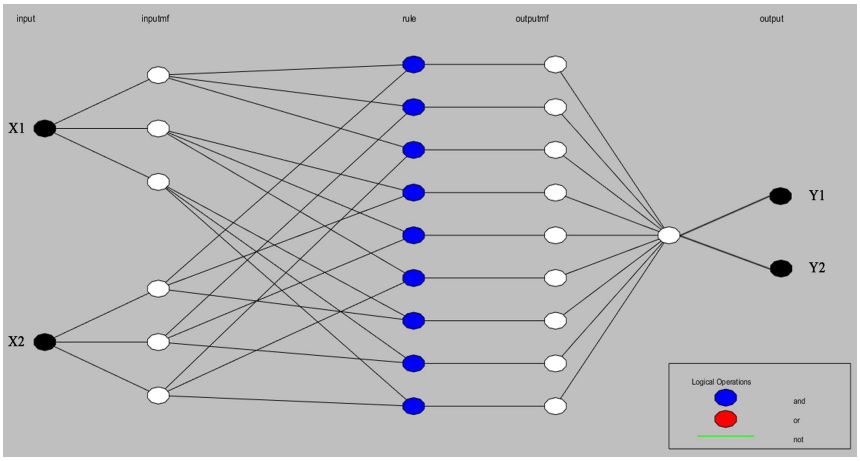

Figure 10. Network architecture of ANFIS modelling.

Figure 13, Figure 14, Figure 15, and Figure 16 illustrate the relation between measured (target) and predicted (output) Y1 and Y2 based on both Gyratory compactor and Marshall method. From the Figures, we notice that there is a good correlation coefficient in both training and validation data with, R= 0, 9927 for Y1 and R = 0.9962 for Y2 based on Gyratory compactor. Furthermore, the findings indicated a high performance results in Marshall method with, R= 0, 9993 for Y1 and R = 0.9977 for Y2. The latter indicated that the proposed ANFIS model in this study give high performance results, and closer to the experimental ones.

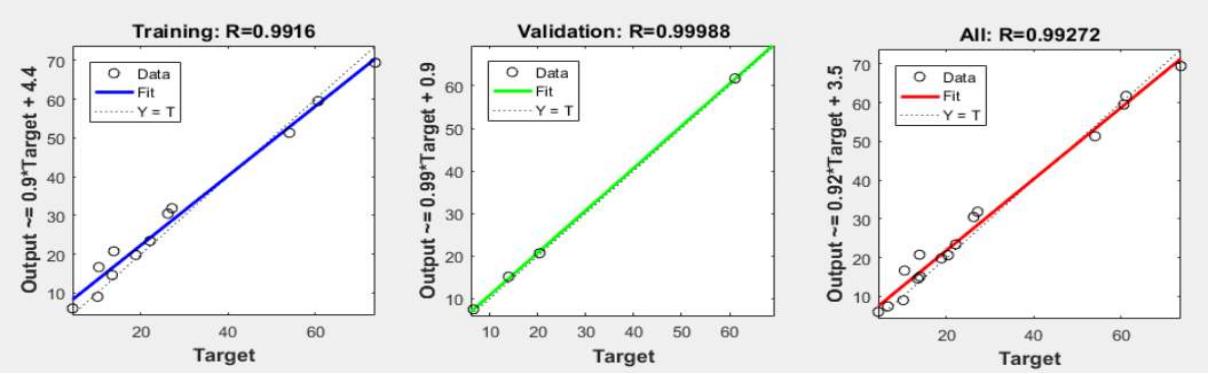

Figure 11. Relation between predicted and measured Y1 based on Gyratory compactor using ANFIS.

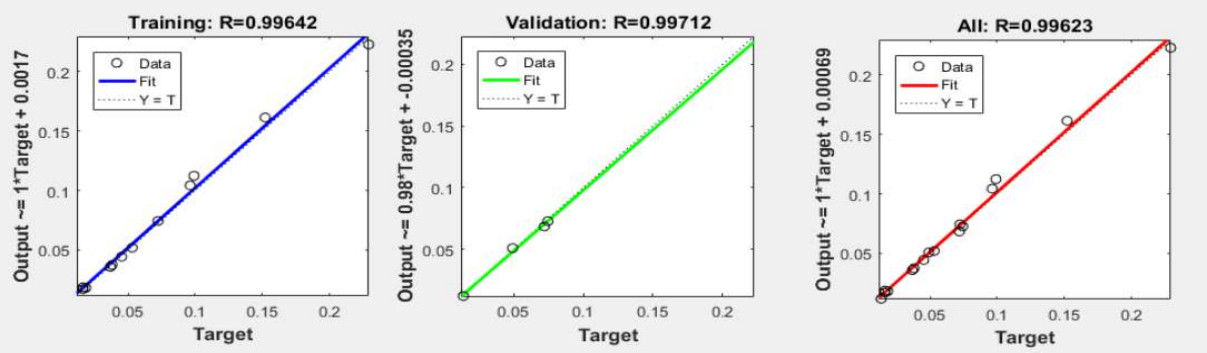

Figure 12. Relation between predicted and measured Y2 based on Gyratory compactor using ANFIS.

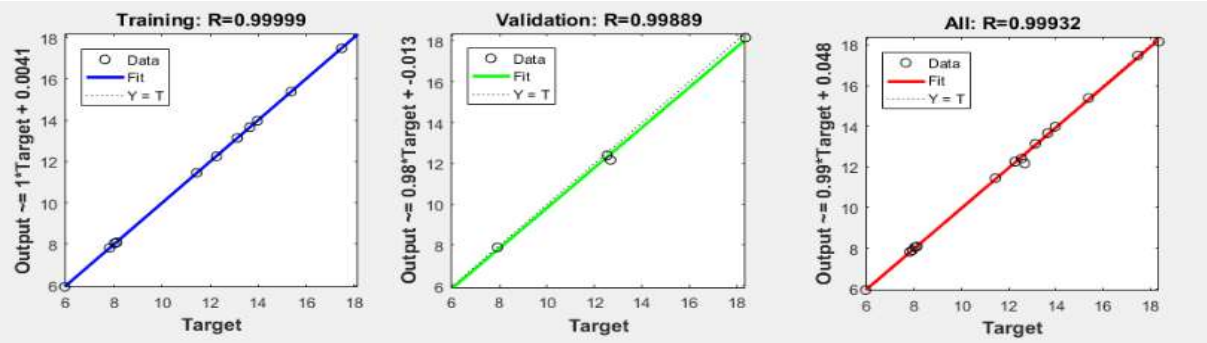

Figure 13. Relation between predicted and measured Y1 based on Marshall method using ANFIS.

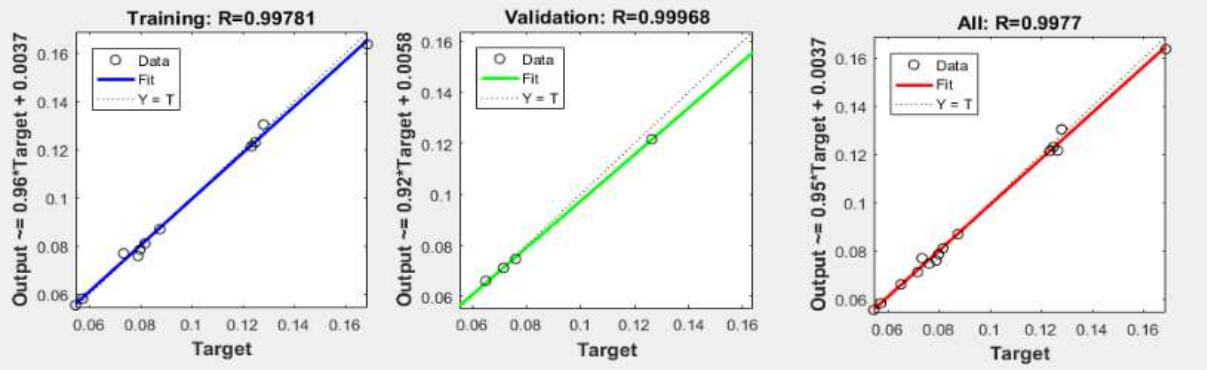

Figure 14. Relation between predicted and measured Y2 based on Marshall method using ANFIS.

4.4 Comparison between machine learning methods

To identify the optimal machine learning model, the process begins with selecting input parameters that significantly influence the target values. The second step involves determining the most suitable machine learning method. Initially, both ANN and ANFIS models were evaluated for predicting Y1 and Y2 based on four statistical performance metrics. Table 5 summarizes the performance of each model using the selected optimal input parameters during the training and validation phases. The four metrics used to compare the models were Mean Square Error (MSE), Root Mean Square Error (RMSE), the coefficient of determination (R2), and the Pearson correlation coefficient (R). The dataset was split into 80% for training and 20% for validation. As shown in Table 5, the machine learning methods were applied to model the target values, with their parameters fixed and evaluated based on the performance metrics to determine the best model. For the ANN method, the metrics ranged as follows: MSE (0.1948 to 16.8239), RMSE (0.4414 to 4.1017), R (0.9086 to 0.9993), and R2 (0.8256 to 0.9987). Similarly, for the ANFIS model, the results were MSE (0.0367 to 11.5213), RMSE (0.1915 to 3.3943), RRR (0.9916 to 0.9999), and R2R^2R2 (0.9833 to 0.9998). The findings

indicate that the ANFIS model achieved the best performance, demonstrating the highest accuracy in predicting Y1 and Y2 during both the training and validation phases for the Gyratory Compactor and Marshall methods. The ANN model ranked second, providing acceptable accuracy but slightly lower than ANFIS. These results highlight the superior performance of the ANFIS model for this application.

Table 4. Performance indicators values of the machine learning models.

			ANN				ANFIS			
		Data	MSE	RMSE	R	R2	MSE	RMSE	R	R2
Gyratory compactor	Y1	Train	1.5171	1.2317	0.9868	0.9737	1.3278	1.1523	0.9916	0.9833
		Validation	8.8762	2.9793	0.9581	0.9180	0.0415	0.2037	0.9999	0.9998
		All	2.8968	1.7020	0.9764	0.9535	1.0486	1.0240	0.9927	0.9855
	Y2	Train	16.8239	4.1017	0.9820	0.9643	11.4593	3.3852	0.9964	0.9929
		Validation	10.5593	3.2495	0.9993	0.9987	11.2325	3.3515	0.9971	0.9942
		All	15.6491	3.9559	0.9840	0.9682	11.5213	3.3943	0.9962	0.9925
Marshal	Y1	Train	0.1948	0.4414	0.9953	0.9906	0.0367	0.1915	0.9999	0.9998
		Validation	7.4595	2.7312	0.9585	0.9187	0.0562	0.2371	0.9989	0.9978
		All	1.5570	1.2478	0.9607	0.9230	0.0474	0.2177	0.9993	0.9986
	Y2	Train	0.9807	0.9903	0.9667	0.9345	0.2084	0.4565	0.9978	0.9956
		Validation	3.7756	1.9431	0.9086	0.8256	0.1809	0.4253	0.9997	0.9994
		All	1.5048	1.2267	0.9498	0.9021	0.2099	0.4581	0.9977	0.9954

5 Discussion

The present study revealed several key findings regarding the effect of rubber on the creep behavior of asphalt mixtures. Firstly, it was observed that incorporating a low percentage of rubber (0.25%) significantly improved creep modulus and reduced deformation at both 20°C and 60°C. This enhancement is attributed to the presence of zinc oxide in the rubber, which acts as a particle-agglomerating agent, strengthening the bond between the mixture components. However, higher percentages of rubber (0.5% and 0.75%) led to a decrease in creep modulus and an increase in deformation, likely due to the presence of unabsorbed rubber particles that disrupt the binder continuity. Secondly, the study demonstrated that the compaction method significantly influenced the creep behavior. Samples compacted with the gyratory compactor exhibited lower axial deformations and higher creep modulus compared to those compacted with the Marshall Method. Finally, the machine learning models, particularly the ANFIS model, demonstrated excellent predictive capabilities for creep modulus and creep compliance. The ANFIS model outperformed the ANN model in terms of accuracy and precision, providing a valuable tool for engineers to predict the performance of rubber modified asphalt mixtures without the need for extensive laboratory testing. The findings of this study are consistent with previous research that has shown that incorporating low percentages of certain additives can enhance the performance of asphalt mixtures. For example, studies on the use of polyethylene terephthalate (PET) have demonstrated improvements in fatigue behavior and reductions in stiffness [11]. Similarly, studies on the use of waste plastic and rubber have shown increases in strength and resistance to permanent deformation [12]. However, the specific effects and optimal dosages of additives can vary depending on the type of additive, the compaction method, and the testing conditions.

The findings of this study have significant implications for the design and construction of sustainable pavements. By utilizing rubber, a waste material, as a modifier for asphalt mixtures, we can reduce environmental pollution and promote the circular economy. The optimal dosage of rubber, as identified in this study, can be used to optimize mixture design and enhance pavement performance. Furthermore, the developed machine learning models can be used as a predictive tool to assist engineers in selecting the most suitable mixture design for specific traffic and environmental conditions. One of the strengths of this study is the comprehensive investigation of the effect of rubber on the creep behavior of asphalt mixtures, considering different percentages of rubber, two compaction methods, and two temperature levels. Additionally, the use of

advanced machine learning techniques, such as ANFIS, provides a robust framework for predicting the performance of these mixtures. However, there are also some limitations to this study.

The study focused on a limited range of rubber percentages. Further research is needed to investigate a wider range of percentages and to explore the effects of different types of rubber. Additionally, the study only considered two compaction methods. Future research could investigate the effects of other compaction methods, such as roller compaction, on the creep behavior of modified asphalt mixtures. Finally, this study demonstrates that incorporating a low percentage of rubber (0.25%) into asphalt mixtures can significantly enhance their creep resistance and improve their overall performance. The ANFIS model has proven to be a valuable tool for predicting the creep behavior of these mixtures, offering a more efficient and accurate approach compared to traditional methods. Future research should focus on investigating the long-term performance of rubber modified asphalt mixtures in real-world conditions, considering factors such as traffic loading, environmental aging, and moisture susceptibility. Additionally, exploring the use of other waste materials and developing more sophisticated machine learning models could further advance the field of sustainable pavement engineering.

6 Conclusion

This study investigated the influence of rubber on the creep behavior of asphalt mixtures, aiming to enhance their mechanical performance while promoting environmental sustainability. The findings demonstrate that incorporating a low percentage of rubber (0.25%) can significantly enhance creep resistance, as evidenced by increased creep modulus and reduced deformation at both 20°C and 60°C. This improvement is attributed to the strengthening effect of the rubber on the binder-aggregate interface. However, higher percentages of rubber (0.5% and 0.75%) led to a decrease in creep modulus and an increase in deformation, indicating potential detrimental effects on mixture performance. Furthermore, the study highlights the significant influence of compaction methods on the creep behavior of asphalt mixtures. Samples compacted with the gyratory compactor exhibited superior creep resistance (lower deformations and higher stiffness) compared to those compacted with the Marshall Method. This finding emphasizes the critical role of compaction method in determining the creep behavior of modified asphalt mixtures. The study successfully demonstrated the effectiveness of machine learning techniques, particularly the ANFIS model, in predicting creep modulus and compliance. The high accuracy and precision of the ANFIS model offer a valuable tool for engineers to optimize mixture design and predict pavement performance more efficiently. Based on these findings, it can be concluded that 0.25% rubber content is the most effective in improving creep resistance while maintaining desirable mechanical properties. Gyratory compaction generally resulted in superior creep performance compared to Marshall compaction. However, the choice of compaction method should be carefully considered based on specific project requirements and available equipment. The developed ANFIS model provides a powerful tool for optimizing mixture design, predicting pavement performance, and reducing the reliance on extensive laboratory testing. Future research should focus on investigating the long-term performance of rubber modified asphalt mixtures in real-world conditions, considering factors such as traffic loading, environmental aging, and moisture susceptibility. Exploring the use of different types of rubber and other waste materials as modifiers for asphalt mixtures is also crucial. Furthermore, developing more sophisticated machine learning models, incorporating additional parameters and considering the effects of long-term aging and environmental factors, can further advance the field of sustainable pavement engineering.

References

[1] A. Behnood et M. Modiri Gharehveran, « Morphology, rheology, and physical properties of polymer-modified asphalt binders », *Eur. Polym. J.*, vol. 112, p. 766-791, mars 2019, doi: 10.1016/j.eurpolymj.2018.10.049.

[2] K. Zhang, Wei Xie, et Y. Zhao, « Permanent deformation characteristic of asphalt mixture under coupling effect of moisture, overload and loading frequency », *Constr. Build. Mater.*, vol. 272, p. 121985, févr. 2021, doi: 10.1016/j.conbuildmat.2020.121985.

[3] B. W. Al-Mistarehi, Y. T. Obaidat, T. S. Khedaywi, et A. T. Al-smadi, « Behavior of Modified Asphalt Using Polystyrene Concrete in Static Creep: Experimental and Numerical Study », *Iran. J. Sci. Technol. Trans. Civ. Eng.*, vol. 46, nº 3, p. 2359-2367, juin 2022, doi: 10.1007/s40996-022-00866-1.

[4] M. A. Khasawneh, M. M. Taamneh, et O. Albatayneh, « Evaluation of static creep of FORTA-FI strengthened asphalt mixtures using experimental, statistical and feed-forward back-propagation ANN techniques », *Int. J. Pavement Res. Technol.*, vol. 12, nº 1, p. 43-53, janv. 2019, doi: 10.1007/s42947-019-0006-3.

[5] F. R. Safi, K. Hossain, S. Wu, I. L. Al-Qadi, et H. Ozer, « A model to predict creep compliance of asphalt mixtures containing recycled materials », *Constr. Build. Mater.*, vol. 184, p. 374-381, sept. 2018, doi: 10.1016/j.conbuildmat.2018.06.232.

[6] T. O. D. Silva, H. N. Pitanga, M. H. R. Rodrigues, J. D. P. Rezende, G. L. D. O. Marques, et F. D. A. Simões, « Study of the mechanical behavior of asphalt mixtures in terms of creep and Superpave compaction parameters », *Acta Sci. Technol.*, vol. 45, p. e60212, août 2022, doi: 10.4025/actascitechnol.v45i1.60212.

[7] N. Usman et M. I. M. Masirin, « Performance of asphalt concrete with plastic fibres », in *Use of Recycled Plastics in Eco-efficient Concrete*, Elsevier, 2019, p. 427-440. doi: 10.1016/B978-0-08-102676-2.00020-7.

[8] B. Saoudi et S. Haddadi, « Predicting creep deformation of asphalts modified with polymer using artificial neural networks », 2021, doi: 10.34910/MCE.101.6.

[9] M. Mazouz et M. Merbouh, « The Effect of Low-Density Polyethylene Addition and Temperature on Creep-recovery Behavior of Hot Mix Asphalt », *Civ. Eng. J.*, vol. 5, nº 3, p. 597, mars 2019, doi: 10.28991/cej-2019-03091271.

[10] E. I. Alrashydah et S. A. Abo-Qudais, « Modeling of creep compliance behavior in asphalt mixes using multiple regression and artificial neural networks », *Constr. Build. Mater.*, vol. 159, p. 635-641, janv. 2018, doi: 10.1016/j.conbuildmat.2017.10.132.

[11] A. Zofka et I. Yut, « Prediction of Asphalt Creep Compliance Using Artificial Neural Networks », *Arch. Civ. Eng.*, vol. 58, nº 2, p. 153-173, juin 2012, doi: 10.2478/v.10169-012-0009-9.

[12] J. Liu et J. Liu, « Prediction models for low-temperature creep compliance of asphalt mixtures containing reclaimed asphalt pavement (RAP) », *Constr. Build. Mater.*, vol. 306, p. 124915, nov. 2021, doi: 10.1016/j.conbuildmat.2021.124915.

[13] A. Roshan et M. Abdelrahman, « Predicting Flexural-Creep Stiffness in Bending Beam Rheometer (BBR) Experiments using Advanced Super Learner Machine Learning Techniques », *Res. Eng. Struct. Mater.*, vol. 10, nº 3, p. 1195-1208, juin 2024, doi: 10.17515/resm2024.58me1027rs.

[14] R. Gogoi, K. P. Biligiri, et N. C. Das, « Performance prediction analyses of styrene-butadiene rubber and crumb rubber materials in asphalt road applications », *Mater. Struct.*, vol. 49, nº 9, p. 3479-3493, sept. 2016, doi: 10.1617/s11527-015-0733-0.

[15] D. Lo Presti, « Recycled Tyre Rubber Modified Bitumens for road asphalt mixtures: A literature review », *Constr. Build. Mater.*, vol. 49, p. 863-881, déc. 2013, doi: 10.1016/j.conbuildmat.2013.09.007.

[16] L. Sadoudi, R. Mitiche-Kettab, et D. S. Bachir, « Evaluation of the workability, marshall parameters, and the stiffness modulus of rubber modified bituminous concrete », *Int. J. Sustain. Build. Technol. Urban Dev.*, vol. 10, nº 2, p. 43-55, juin 2019, doi: 10.22712/susb.20190006.

[17] L. da Silva, A. Benta, et L. Picado-Santos, « Asphalt rubber concrete fabricated by the dry process: Laboratory assessment of resistance against reflection cracking », *Constr. Build. Mater.*, vol. 160, p. 539-550, janv. 2018, doi: 10.1016/j.conbuildmat.2017.11.081.

[18] H. T. Tai Nguyen et T. Nhan Tran, « Effects of crumb rubber content and curing time on the properties of asphalt concrete and stone mastic asphalt using dry process », *Int. J. Pavement Res. Technol.*, vol. 11, nº 3, p. 236-244, mai 2018, doi: 10.1016/j.ijprt.2017.09.014.

[19] J. L. Feiteira Dias, L. G. Picado-Santos, et S. D. Capitão, « Mechanical performance of dry process fine crumb rubber asphalt mixtures placed on the Portuguese road network », *Constr. Build. Mater.*, vol. 73, p. 247-254, déc. 2014, doi: 10.1016/j.conbuildmat.2014.09.110.

[20] B. Amin, « Predicting Shear Stress Parameters in Consolidated Drained Conditions Using Artificial Intelligence Methods », *Basic Appl. Sci. - Sci. J. King Faisal Univ.*, vol. 22, nº 1, p. 1-7, 2021, doi: 10.37575/b/sci/0069.

[21] N. E.-I. Bioud, I. O. Laid, et M. A. Benbouras, « Estimating the fundamental period of infilled RC frame structures via deep learning », *Urb. Arhi. Const*, vol. 14, nº 1, p. 59-73, 2023.

[22] M. A. Benbouras, L. Sadoudi, et A. Leghouchi, « Prediction of the resilient modulus of subgrade soil using machine-learning techniques », *Urb. Arch. Cons*, vol. 16, nº 1, p. 87-104, 2025.

[23] S. Alioua, A. Arab, M. A. Benbouras, et A. Leghouchi, « Modeling Static Liquefaction Susceptibility of Saturated Clayey Sand using Advanced Machine-Learning techniques », *Transp. Infrastruct. Geotechnol.*, vol. 11, nº 5, p. 2903-2931, oct. 2024, doi: 10.1007/s40515-024-00396-5.

[24] F. Debiche, M. A. Benbouras, A.-I. Petrisor, L. M. Baba Ali, et A. Leghouchi, « Advancing Landslide Susceptibility Mapping in the Medea Region Using a Hybrid Metaheuristic ANFIS Approach », *Land*, vol. 13, nº 6, p. 889, juin 2024, doi: 10.3390/land13060889.

[25] A. Fouchal, Y. Tikhamarine, M. A. Benbouras, D. Souag-Gamane, et S. Heddam, « Biological oxygen demand prediction using artificial neural network and random forest models enhanced by the neural architecture search algorithm », *Model. Earth Syst. Environ.*, vol. 11, nº 1, p. 9, févr. 2025, doi: 10.1007/s40808-024-02178-x.

[26] A. H. Y. Habal et M. A. Benbouras, « California bearing ratio and compaction parameters prediction using advanced hybrid machine learning methods », *Asian J. Civ. Eng.*, vol. 26, nº 1, p. 121-146, janv. 2025, doi: 10.1007/s42107-024-01179-6.